University of Windsor
Scholarship at UWindsor

Electronic Theses and Dissertations | Theses, Dissertations, and Major Papers

1-1-1967

A Time of Flight Mass Spectrometer.

Nicolas Finney
University of Windsor

Follow this and additional works at: https://scholar.uwindsor.ca/etd

Recommended Citation
Finney, Nicolas, "A Time of Flight Mass Spectrometer." (1967). *Electronic Theses and Dissertations*. 6474.
https://scholar.uwindsor.ca/etd/6474

This online database contains the full-text of PhD dissertations and Masters' theses of University of Windsor students from 1954 forward. These documents are made available for personal study and research purposes only, in accordance with the Canadian Copyright Act and the Creative Commons license—CC BY-NC-ND (Attribution, Non-Commercial, No Derivative Works). Under this license, works must always be attributed to the copyright holder (original author), cannot be used for any commercial purposes, and may not be altered. Any other use would require the permission of the copyright holder. Students may inquire about withdrawing their dissertation and/or thesis from this database. For additional inquiries, please contact the repository administrator via email (scholarship@uwindsor.ca) or by telephone at 519-253-3000ext. 3208.

A TIME OF FLIGHT MASS SPECTROMETER

by

Nicolas Finney

A Thesis
Submitted to the Faculty of Graduate Studies through the Department of Physics in Partial Fulfillment of the Requirements for the Degree of Master of Science at the University of Windsor.

Windsor, Ontario

1967

Reproduced with permission of the copyright owner. Further reproduction prohibited without permission.

UMI Number: EC52655

INFORMATION TO USERS

The quality of this reproduction is dependent upon the quality of the copy submitted. Broken or indistinct print, colored or poor quality illustrations and photographs, print bleed-through, substandard margins, and improper alignment can adversely affect reproduction.

In the unlikely event that the author did not send a complete manuscript and there are missing pages, these will be noted. Also, if unauthorized copyright material had to be removed, a note will indicate the deletion.

UMI®

UMI Microform EC52655

Copyright 2008 by ProQuest LLC.

All rights reserved. This microform edition is protected against unauthorized copying under Title 17, United States Code.

ProQuest LLC
789 E. Eisenhower Parkway
PO Box 1346
Ann Arbor, MI 48106-1346

Reproduced with permission of the copyright owner. Further reproduction prohibited without permission.

ABA 3173

Approved

A van Wijngaarden

Dr. A. van Wijngaarden
(Supervisor)

N E Hedgecock

Dr. N. E. Hedgecock

J. Huschilt

Dr. J. J. Huschilt

177770

Reproduced with permission of the copyright owner. Further reproduction prohibited without permission.

Abstract

A new, non-magnetic Time of Flight Mass Spectrometer has been constructed. Preliminary work with this instrument indicates that the theoretical mass resolution formula, previously derived by Lum, 1964, is in error. New mass resolution formulae which agree with experimental observations, are presented. These formulae distinguish between even and odd n numbers. A resolution of one part in six thousand has been achieved with the instrument. Although higher resolutions are theoretically possible, they have not been reached due to a splitting of the mass peaks when large R.F. voltages are applied to the deflecting plates. Several possible causes of this splitting are advanced, but no detailed investigation of the effect has been done to date.

Reproduced with permission of the copyright owner. Further reproduction prohibited without permission.

Acknowledgements

I would like to express my gratitude to Dr. A. van Wijngaarden for his supervision, his friendship, and the freedom he has extended to me during the course of this work. I would also like to thank Mr. L. Hastings for his helpful suggestions, and Mr. Grewe for the work performed in the Physics Machine Shop.

Reproduced with permission of the copyright owner. Further reproduction prohibited without permission.

TABLE OF CONTENTS

ABSTRACT i

ACKNOWLEDGEMENTS ii

LIST OF FIGURES iv

CHAPTER I - INTRODUCTION

A. Mass Spectroscopy 1
B. Operating Principles 2

CHAPTER II - THEORY

A. Theoretical Mass Resolution 6

CHAPTER III - APPARATUS AND TECHNIQUE

A. Introduction 15
B. Adjustable Slits and R.F. Deflecting Plates 15
C. Radio Frequency Supply 18
D. High Voltage System 21
E. Particle Detection 23

CHAPTER IV - EXPERIMENTAL RESULTS

A. Slow Voltage Sweeping 24
B. Fast Voltage Sweeping 24
C. Frequency Sweep, High Power Oscillator 26
D. Frequency Sweep, Low Power Oscillator 26
E. General Results 29

CHAPTER V - DISCUSSION AND CONCLUSION 34

BIBLIOGRAPHY 36

VITA AUCTORIS 37

Reproduced with permission of the copyright owner. Further reproduction prohibited without permission.

LIST OF FIGURES

I	Schematic Diagram of the Time of Flight Mass Spectrometer	3
II	Ion Paths in the Mass Spectrometer	11
III	Time of Flight of an Ion Through an R.F. Stage	12
IV	Mass Resolution Criterion	12
V	First R.F. Assembly	16
VI	R.F. Distribution System	20
VII	Slow Voltage Sweeping Circuit	20
VIII	Fast Voltage Sweeping Circuit	22
IX	Recorder Trace for the Slow Voltage Sweeping	25
X	Recorder Trace for Frequency Sweeping with the High Power Oscillator	27
XI	Recorder Trace for Frequency Sweeping with the Low Power Oscillator	28
XII	Recorder Trace for Frequency Sweeping with the Low Power Oscillator showing Peak Splitting	30
XIII	Recorder Trace of Mass Peak Overlapping	31
XIV	Recorder Trace showing the Different Mass Resolution for Even and Odd n Numbers	31
XV	Recorder Trace for a Voltage and a Frequency Sweep showing Comparable Resolutions under the same Conditions	32

Reproduced with permission of the copyright owner. Further reproduction prohibited without permission.

CHAPTER I

INTRODUCTION

A. Mass Spectroscopy

Traditionally, mass measurements have been made (see Duckworth, 1958) with large magnetic deflection type instruments. In such instruments, ion beams of either constant energy or constant velocity are separated into different trajectories corresponding to the different masses present in the beam. For the accurate comparison of two masses, the magnetic field should be the same over both trajectories. Since it is difficult to produce a uniform magnetic field over a large region, such comparisons are limited to ions whose masses are almost equal. This so called doublet method may be used to compare the mass of a heavy ion to the carbon standard, but it is often necessary to employ several intermediate doublet determinations. Hence, the error in the comparison will be the sum of the errors in each of the doublet determinations. Thus an instrument which would permit the direct comparison of two widely separated masses is of great importance.

Smythe and Mattauch in 1932 were the first to use a non-magnetic time of flight instrument to determine atomic masses. Since that time many instruments of this type have been built, but all of them suffer from low resolution, with the possible exception of the electric quadrupole mass spectrometer. These instruments are not suited for the direct determination of large mass differences since a wide range scan must be made between the light and heavy masses. In 1964, Lum reported on a high resolution, non-magnetic Time of Flight Mass Spectrometer.

Reproduced with permission of the copyright owner. Further reproduction prohibited without permission.

This spectrometer, which permits the direct comparison of light and heavy masses, is essentially a velocity filter for a mono-energetic beam of ions. The preliminary operation of a more sophisticated instrument will be discussed in this thesis, and a more accurate theory for the mass resolution will be worked out.

B. Operating Principles

Figure I is a schematic diagram of the Time of Flight Mass Spectrometer. Ions are produced in a surface ionization source (Inghram and Hayden, 1954) and then accelerated towards the ground slit by the high voltage power supply. Ions which are able to pass through the ground slit form an ion beam, represented by the dashed line in the diagram. This beam, after passing sucessively through the first collimating stage, the first R.F. stage, the second collimating stage, the second R.F. stage, and the third collimating stage, enters the detecting system consisting of a magnetic mass analyser and a particle detector. The two R.F. stages produce sinusoidally varying electric fields of the same frequency and amplitude, perpendicular to the ion beam. Only those ions that pass the R.F. stages at zero field can enter the detecting system. Hence, any ion that is detected, must have travelled the distance between the two R.F. stages in an integral number of half periods of the applied frequency. The condition for an ion reaching the detector is

$$v = 2Lf/n \qquad \text{I-1}$$

where v is the velocity of the ion, f is the applied frequency, n is the integral number of half periods, and L is the distance between the two R.F. stages.

Reproduced with permission of the copyright owner. Further reproduction prohibited without permission.

Reproduced with permission of the copyright owner. Further reproduction prohibited without permission.

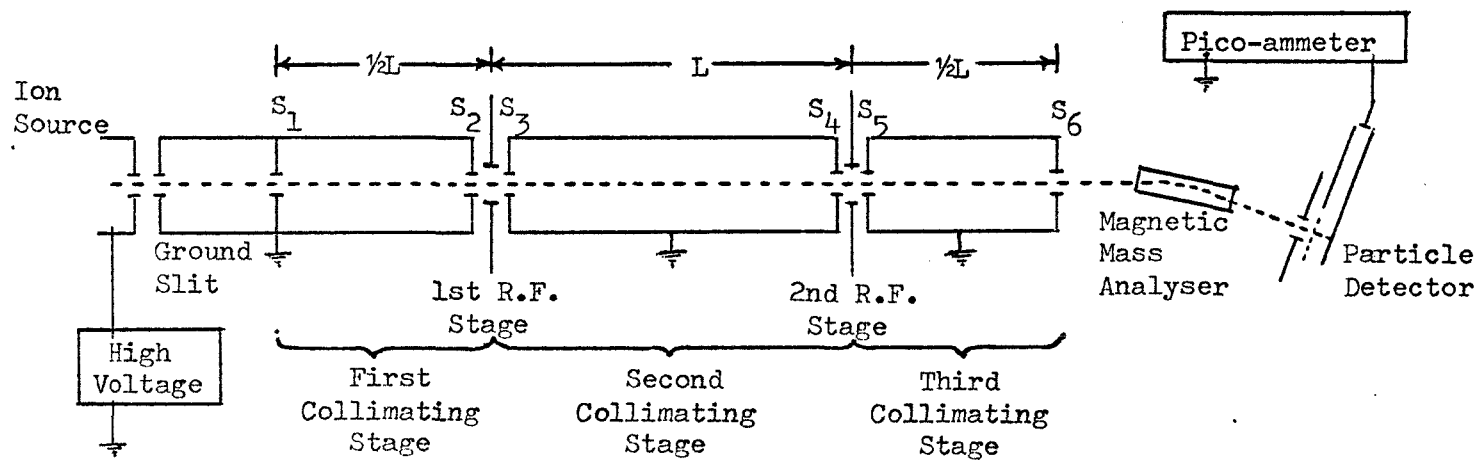

Figure I. A Schematic Diagram of the Time of Flight Mass Spectrometer

Using the principle of the conservation of energy, for an ion starting at rest in the ion source and being accelerated by a potential of V volts, the velocity can be eliminated from Eq. I-1, giving upon rearrangement, an expression for the mass of the detected ion in terms of the parameters of the Time of Flight Mass Spectrometer.

$$m = n^2 eV/2L^2 f^2 \qquad \text{I-2}$$

where m is the mass of the ion and e its charge.

In practice, either the frequency or the voltage is varied, and the ions of mass m will be detected for successive n numbers corresponding to the particular values of the frequency or voltage that satisfy Eq. I-2. Since mass differences rather than absolute masses are measured in practice, the output of the detector versus frequency or voltage can be used to determine these mass differences. When the frequency is varied (frequency sweeping), the mass difference, Δm, between two ions of mass m and $m+\Delta m$, relative to the mass m, is

$$\Delta m/m \simeq 2\Delta f/f \qquad \text{I-3}$$

where Δf is the difference in frequency between the two peaks, provided that the n numbers are the same for the two peaks. If they are not, then Eq. I-3 becomes

$$\Delta m/m \simeq 2\Delta f/f + 2\Delta n/n \qquad \text{I-3a}$$

where Δn is the difference in the n numbers.

Similar expressions for voltage sweeping are

$$\Delta m/m = \Delta V/V \qquad \text{I-4}$$

Reproduced with permission of the copyright owner. Further reproduction prohibited without permission.

and $$\Delta m/m \simeq \Delta V/V + 2\Delta n/n \qquad \text{I-4a}$$

where ΔV is the voltage separation of the two peaks.

For preliminary work with the Time of Flight Mass Spectrometer, it is convenient to use only a small portion of the mass spectrum, since the mass peaks from different parts of the mass spectrum start to overlap at high n numbers. A low resolution magnetic mass analyser is used to select the ions in the desired mass range before detection.

Reproduced with permission of the copyright owner. Further reproduction prohibited without permission.

CHAPTER II

THEORY

A. Theoretical Mass Resolution

The mass resolution for this type of Time of Flight Mass Spectrometer has been derived previously (Lum, 1964) and is given by

$$\Delta m/m = (16Vwb)/(n\pi V_y hL) \qquad \text{II-1}$$

where w is the width of the collimating slits, b is the distance between the R.F. plates, V_y is the amplitude of the R.F. voltage, and h is the length of the R.F. plates in the direction of the ion beam. This equation predicts that the resolution improves linearly with n.

When the frequency or voltage is swept, the same mass will be detected at regular frequency or voltage intervals corresponding (see Eq. I-2) to successive n numbers. In experiments to be described in IV,E, it was observed that peaks for the same mass were alternately "good" and "bad" in resolution for odd and even n respectively. This effect, which is not predicted by Eq. I-1, will now be discussed, and different mass resolution formulae for even and odd n will be derived.

For this purpose, the range, $\Delta\tau$, in the time of flight of an ion about an average time of flight, τ, will be investigated. Time zero is defined as the time when the R.F. field is zero while an ion is passing through an R.F. stage. The times that an ion enters and emerges from an R.F. stage are defined as t_i and t_f respectively. An ion that did not undergo an angular deflection in passing through an R.F. stage, must have entered the stage at time $-h/2v$ and emerged at time $+h/2v$. However,

Reproduced with permission of the copyright owner. Further reproduction prohibited without permission.

this ion does suffer a displacement, and leaves the R.F. stage moving parallel to its original direction. This displacement is proportional to V_y and is usually negligible compared to the slit widths. If an ion passes both R.F. stages with no angular deflection in either one, it must have travelled the distance between the R.F. stages in an integral number of half periods of the applied frequency.

$$\tau = nT/2 \qquad \text{II-2}$$

where T is the period of the applied frequency and τ is the average time of flight.

Since the instrument has finite slit widths, it is possible for the ions to travel at various small angles to the axis of the instrument and still pass through all the slits, if it suffers the right angular deflection at the R.F. stages. An ion, of course, suffers an angular deflection if it enters the R.F. stage at some time other than -h/2v.

The equation of motion in a direction perpendicular to the ion beam, called the y direction, for an ion in an R.F. stage, is given by

$$mdv_y = eV_y \sin\omega t dt/b \qquad \text{II-3}$$

where v_y is the velocity of the ion in the y direction, ω is the angular frequency of the R.F., and t is the time. Since the R.F. field is small during the times under consideration, Eq. II-3 can be re-written as

$$mdv_y = eV_y \omega t dt/b,$$

which upon integration, becomes,

$$v_{yf} - v_{yi} = eV_y \omega (t_f + t_i)(t_f - t_i)/2mb \qquad \text{II-4}$$

Reproduced with permission of the copyright owner. Further reproduction prohibited without permission.

where the subscripts i and f stand for the initial and final values respectively. The quantity (t_f-t_i) is equal to the time of flight (see figure III) of an ion through an R.F. stage. Ie,

$$t_f-t_i = h/v. \qquad \text{II-5}$$

Substitution of Eq. II-5 into Eq. II-4 yields

$$v_{yf}-v_{yi} = eV_y\omega(t_f+t_i)h/2mvb,$$

which can be written in a more convenient form as,

$$v_{yf}-v_{yi} = K(t_f+t_i), \qquad \text{II-6}$$

where $$K = heV_y\omega/2mvb. \qquad \text{II-6a}$$

An entry error time, t', will now be defined as the difference between the time, t_i, that an ion actually enters an R.F. stage and the time,-h/2v, that it should have entered if it were to suffer no angular deflection. Thus

$$t' = t_i + h/2v. \qquad \text{II-7}$$

The value of t' is positive if the ion enters later than -h/2v and negative if earlier. By means of Eqs. II-5, II-6, and II-7, the entry error time can be expressed in terms of the change in y velocity as

$$t' = (v_{yf}-v_{yi})/2K. \qquad \text{II-8}$$

The maximum y velocity that an ion can have upon emerging from one slit and still pass through the next slit, both of width w, is approximately given by

$$v_{y_{max.}} \lessapprox vw/Le \qquad \text{II-9}$$

Reproduced with permission of the copyright owner. Further reproduction prohibited without permission.

where Le is the distance between the two slits.

If the value of the entry error time, t_1', for the first R.F. stage is different from the entry error time, t_2', for the second R.F. stage, then the ion must have travelled the distance between the two R.F. stages in some time other than the average time of flight, τ. The difference, $\Delta t'$, between the actual time of flight and the average time of flight is equal to the difference between the two entry error times,

$$\Delta t' = \left| t_2' - t_1' \right|. \qquad \text{II-10}$$

In the calculation of t_2' care must be taken to distinguish between the even and odd n numbers. For an even n, the K value at the second R.F. stage has the same sign as at the first R.F. stage; whereas, for odd n, the K value has the opposite sign corresponding to a change in the sign of V_y.

Since the three collimating stages are ½L, L, and ½L long, going in the direction of the ion beam, the maximum value of v_y entering the first R.F. stage is $\pm 2vw/L$, leaving the first R.F. stage and entering the second R.F. stage is $\pm vw/L$, and leaving the second R.F. stage is $\pm 2vw/L$.

Table I shows some representative combinations of v_y in the three collimating stages, and the corresponding entry error times for the two R.F. stages as well as the error in the time of flight, $\Delta t'$. The entry error times are calculated from Eq. II-8 and are in units of vw/2KL (see Eqs. II-8 and II-9). The velocities are in units of vw/L. Figure II is a schematic representation of the different ion paths that give rise to the errors listed in table I.

Reproduced with permission of the copyright owner. Further reproduction prohibited without permission.

Table I

1st R.F. Stage			2nd R.F. Stage				Error	
					n even	n odd	n even	n odd
v_{yi}	v_{yf}	t_1'	v_{yi}	v_{yf}	t_2'	t_2'	$\Delta t'$	$\Delta t'$
0	0	0	0	0	0	0	0	0
0	0	0	0	± 2	± 2	∓ 2	2	2
0	± 1	± 1	± 1	0	∓ 1	± 1	2	0
0	± 1	± 1	± 1	∓ 2	∓ 3	± 3	4	2
± 2	0	∓ 2	0	0	0	0	2	2
± 2	0	∓ 2	0	∓ 2	∓ 2	± 2	0	4
± 2	∓ 1	∓ 3	∓ 1	0	± 1	∓ 1	4	2
± 2	∓ 1	∓ 3	∓ 1	± 2	± 3	∓ 3	6	0

The maximum $\Delta t'$ values listed in the last two columns of table I for even and odd n, are 6 and 4 respectively. No other combinations of v_y can produce larger values of $\Delta t'$ for an ion that passes through all the slits and is detected.

The range in the time of flight is equal to twice the maximum error in the time of flight, ie,

$$\Delta \tau = 2\Delta t'. \qquad \text{II-11}$$

The range in the time of flight will now be related to the mass resolution of the instrument. If two singly charged ions of mass m and $m+\Delta m$ are accelerated by the same potential V, then their kinetic energies will be equal. Ie,

$$\tfrac{1}{2}mv^2 = \tfrac{1}{2}(m+\Delta m)v'^2,$$

where v is the velocity of the ion of mass m, and v' is the velocity of the ion of mass $m+\Delta m$. If the mass difference, Δm, is small, then the

Reproduced with permission of the copyright owner. Further reproduction prohibited without permission.

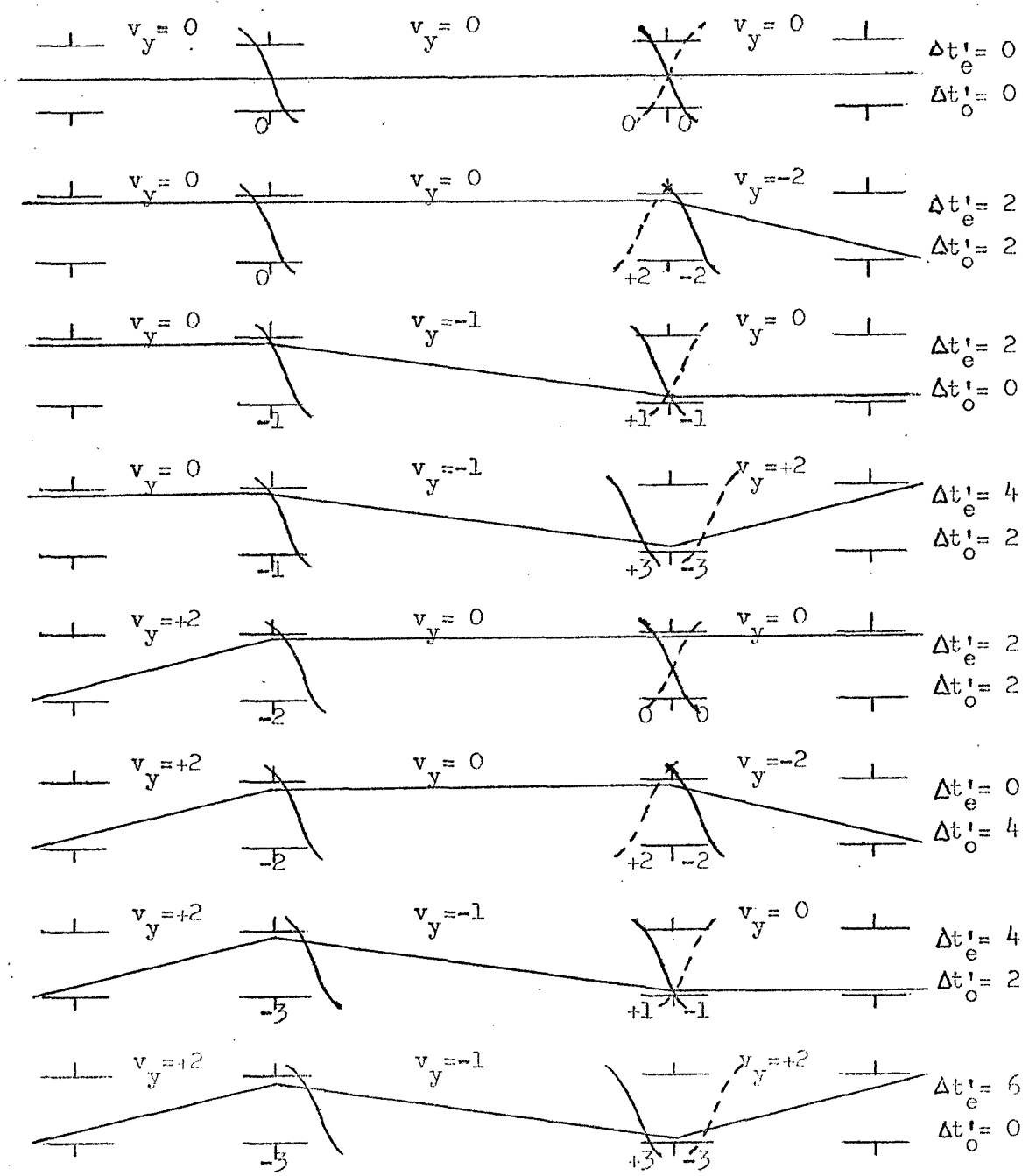

Figure II. This figure shows the paths of the ions through the mass spectrometer for the eight cases listed in table I. The sine waves are superimposed on the R.F. stages to show which part of the R.F. acts on the ions. Only one value of v_y is given since the case for the other value is very similar. These velocities are in units of vw/L. The numbers underneath the R.F. stages are the entry error times, t', in units of vw/2KL. The two cases for the second R.F. stage are indicated, the case for even n being given by the solid sine wave and the case for odd n by the dashed sine wave. The values at the right are the total errors in the time of flight, $\Delta t'$, the subscripts e and o referring to the even and odd cases respectively.

Reproduced with permission of the copyright owner. Further reproduction prohibited without permission.

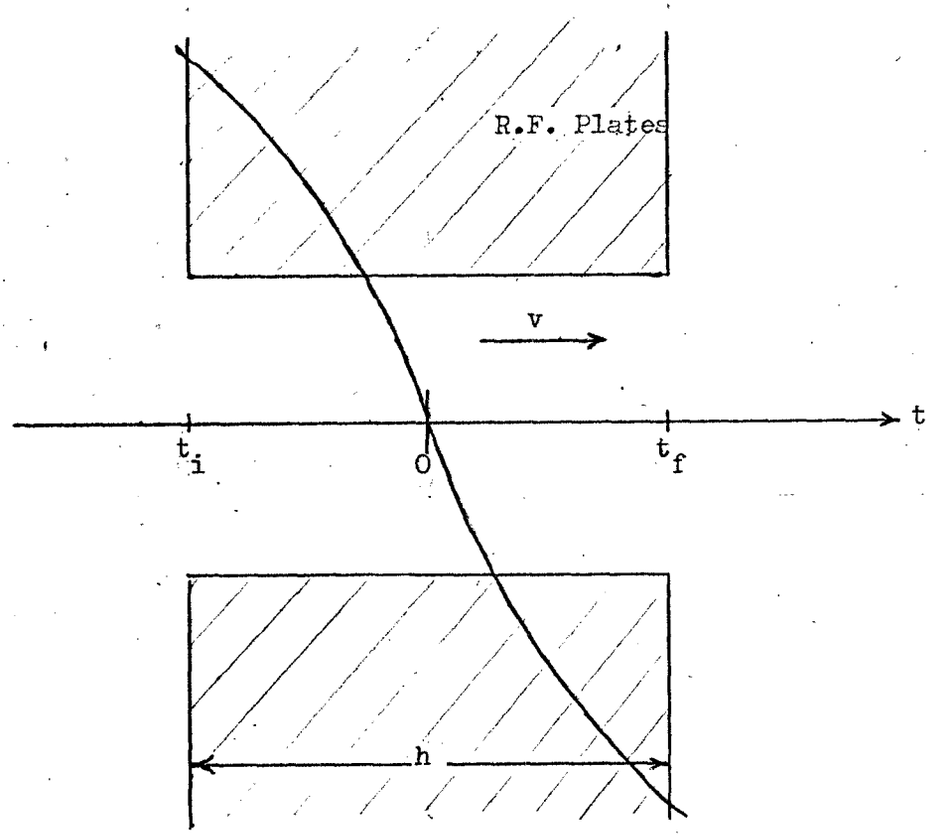

Figure III. Time of Flight of an Ion through an R.F. Stage

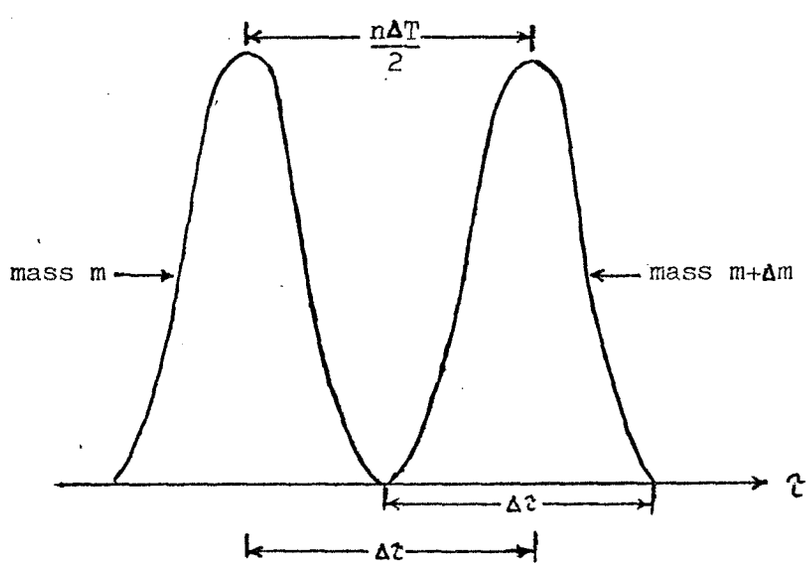

Figure IV. Mass Resolution Criterion

Reproduced with permission of the copyright owner. Further reproduction prohibited without permission.

difference in velocities, $\Delta v = v - v'$, will be small, so that the above equation can be re-written as

$$\Delta m/m \simeq 2\Delta v/v. \qquad \text{II-12}$$

Since the velocity, for an ion that is detected, is related to the frequency as

$$v = 2Lf/n \qquad \text{I-1}$$

and the period is the reciprocal of the frequency, Eq. II-12 becomes

$$\Delta m/m \simeq 2\Delta T/T, \qquad \text{II-13}$$

where ΔT is difference in periods of the two frequencies at which the masses are detected.

Two mass peaks can be resolved at their bases (see figure IV), when the difference in their times of flight, $n\Delta T/2$, is equal to the range in the time of flight, $\Delta\tau$. Thus,

$$\Delta T = 2\Delta\tau/n. \qquad \text{II-14}$$

Then by means of Eqs. II-14, and II-11, Eq. II-13 becomes

$$\Delta m/m \simeq 8\Delta t'/nT. \qquad \text{II-15}$$

Hence, using the two maximum values of $\Delta t'$ from table I, the theoretical mass resolution for even n is

$$\Delta m/m = (48Vwb)/(n\pi V_y hL), \qquad \text{II-16a}$$

and for odd n is

$$\Delta m/m = (32Vwb)/(n\pi V_y hL). \qquad \text{II-16b}$$

Reproduced with permission of the copyright owner. Further reproduction prohibited without permission.

A comparison of Eqs. II-16a and II-16b with Eq. II-1 shows that the resolution of the instrument given by Lum is incorrect by a factor of 2 for the odd peaks and a factor of 3 for the even peaks. The reason for this is that Lum only considered the time interval over which one of the R.F. stages transmits ions through the next collimating stage as the range in the time of flight.

From the definition of mass resolution it can be seen that Eqs. I-3 and I-4 may be used to measure the experimental mass resolution of the instrument when Δf and ΔV are taken as the widths of the peaks at their bases.

Reproduced with permission of the copyright owner. Further reproduction prohibited without permission.

CHAPTER III

APPARATUS AND TECHNIQUE

A. Introduction

In I,B the basic machine layout has been described. The vacuum system containing the source, collimating stages and the R.F. stages consists of six inch drawn brass tubing evacuated by four Edwards E02 vacuum pumps to an ultimate pressure of 1×10^{-6} torr. The source is insulated from the rest of the system by an eight inch length of four inch diameter glass tubing. A low resolution magnetic mass analyser is placed between slit S_6 and the detector. The length of the instrument between slits S_1 and S_6 is approximately 10m., being divided into the first, second, and third collimating stages of approximate lengths 2.5m., 5.0m., and 2.5m. respectively. The R.F. deflecting plates are located in the small regions ($\sim 3.7 \times 10^{-2}$m.) between slits S_2 and S_3, and between slits S_4 and S_5. All the collimating slits and the R.F. deflecting plates are adjustable while the instrument is evacuated. Slits S_1 and S_6 have their own separate adjustments while slits S_2 and S_3 and the R.F. plates between them, the first R.F. assembly, and slits S_4 and S_5 and the R.F. plates between them, the second R.F. assembly, are each adjusted as a unit. The various components of the instrument will now be discussed in greater detail.

B. Adjustable Slits and R.F. Deflecting Plates

In order to align the slit system while the instrument is in operation, externally adjustable slit assemblies were constructed. Figure V is a simplified diagram of the first R.F. assembly, which has

Reproduced with permission of the copyright owner. Further reproduction prohibited without permission.

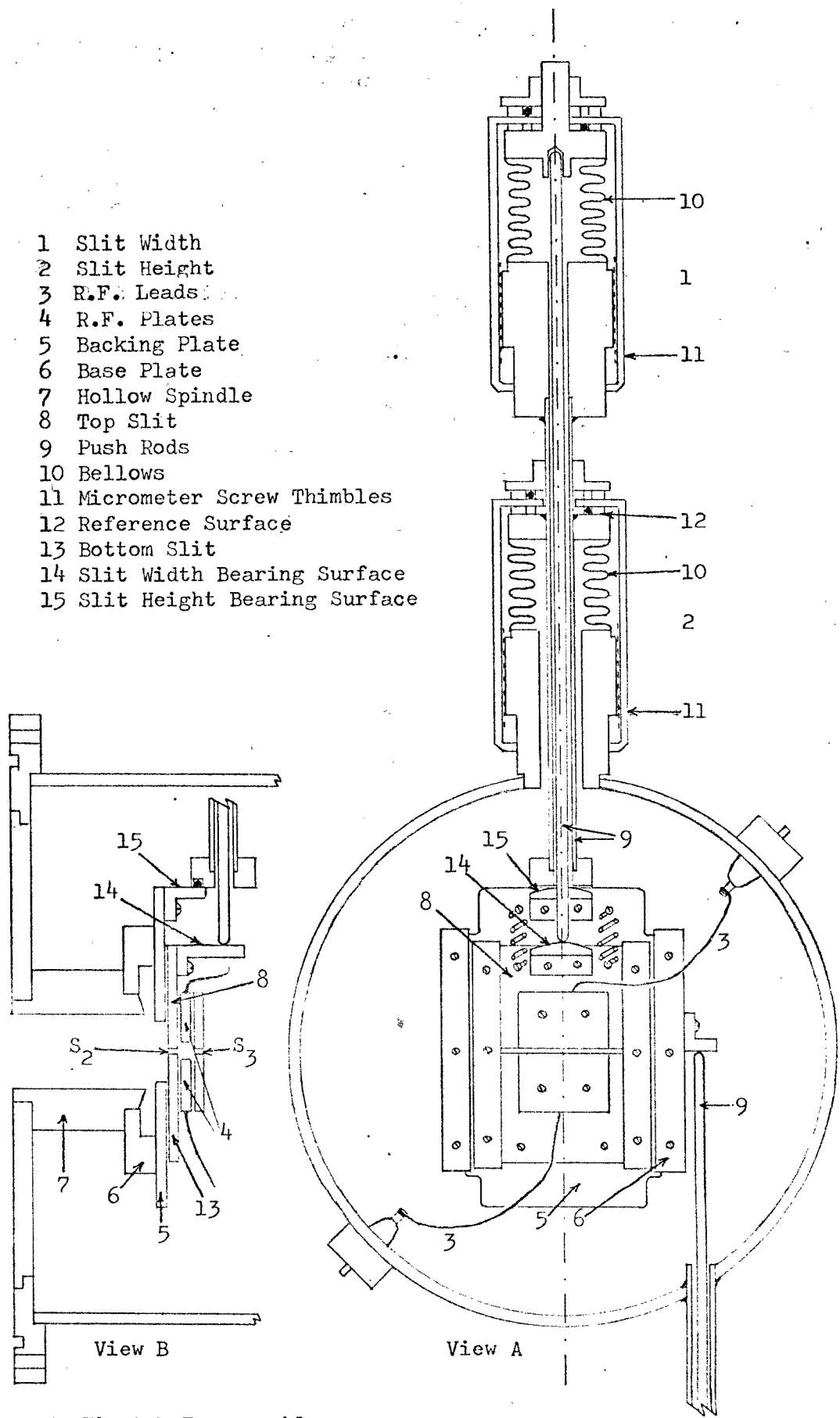

Figure V. First R.F. Assembly

Reproduced with permission of the copyright owner. Further reproduction prohibited without permission.

been designed so that the slits can be moved up and down, rotated, and changed in width. The assembly, see view B, consists of a backing plate, 5, on which is mounted the two halves of slit S_2. The top half of the slit, 8, is mounted so that it is free to slide towards or away from the bottom half of the slit, 13, thus allowing the slit width to be altered. The top R.F. deflecting plate and the top half of slit S_3 are mounted on the top half of slit S_2. Similarly, the bottom R.F. deflecting plate and the bottom half of slit S_3 are mounted on the bottom half of slit S_2. Slits S_2 and S_3 are electrically connected to ground, while the R.F. plates are insulated from ground by means of teflon spacers. The backing plate is mounted on the base plate, 6, so that the entire slit can be moved up or down without changing the slit width. A hollow spindle, 7, is used to support the base plate so that it may be rotated. The ion beam passes along the axis of the spindle and through the slits.

The adjustments for the width, 1, the vertical position, 2, and the rotation are controlled by means of micrometer screw thimbles, see view A. Bellows, 10, are used so that the motion of the micrometer screw thimbles which are on the outside of the vacuum, may be transmitted to the push rods, 9, which are on the inside of the vacuum. These push rods effect the various adjustments of the assembly. Springs are employed to maintain pressure between the push rods and their respective bearing surfaces. As can be seen from the figure, the micrometer screw that adjusts the slit position acts as a reference surface, 12, for the micrometer screw that adjusts the slit width. In this way, the slit width remains constant while the slit position is being adjusted. The bearing surfaces for the push rods that control the the slit width, 14, and the slit position, 15, are curved to allow movement between the push rods and their bearing

Reproduced with permission of the copyright owner. Further reproduction prohibited without permission.

surfaces while the slit is being rotated.

The slit system in figure V is the first R.F. assembly. The second R.F. assembly is constructed in exactly the same manner. Each of the slits S_1 and S_6 is made in a very similar manner except that the R.F. deflecting plates and the second slit in the assembly have been omitted. It should be pointed out that in the R.F. assemblies, the slits on either side of the R.F. deflecting plates serve not only as collimating slits but also as electric field terminating plates. By proper adjustment of the spacing in the R.F. assemblies (Duckworth, 1958), the effective boundary of the R.F. field can be made to coincide with the physical boundary of the R.F. plates.

C. Radio Frequency Supply

The electric fields in the R.F. deflecting stages were produced by an R.F. oscillator whose frequency was approximately 15Mc. Since it is desireable to have the centre of the R.F. deflecting stages at ground potential, it is necessary to apply an R.F. voltage across the upper and lower R.F. plates that is balanced with respect to ground. The output of the R.F. oscillator is unbalanced, making it necessary to insert a balun between the oscillator and the R.F. stages. This balun consists of a half wavelength of coaxial cable, with the input at one end, and the output between the centre conductor at the input end and the centre conductor at the other end. A short electrical connection is made between the ground shields at each end. In order to keep the impedances matched, not only must the balun be fed from a source whose impedance is equal to the characteristic impedance of the cable used to construct the balun, but also the load on the output must have an impedance of four times the

Reproduced with permission of the copyright owner. Further reproduction prohibited without permission.

characteristic impedance of the cable. A schematic diagram of the R.F. distribution system is presented in figure VI. The output of the signal generator was fed by means of a quarter wavelength of cable to an impedance matching network, which provides two outputs of 50Ω each. A half wavelength of cable was used to connect each output to a balun, one balun being used at each R.F. stage. Type RG 58 A/U coaxial cable was used throughout the distribution system.

Two signal sources were used, a low power General Radio bridge oscillator type 1330A, and a high power Colpitts oscillator. The frequency of each of these oscillators could be continuously varied by means of a synchronous motor suitably attached to the tuning section. When the high power oscillator was used, the baluns were terminated by 200Ω, non-inductive power resistors connected across the R.F. plates. When the low power oscillator was used, a different method of terminating the baluns was employed. Since the R.F. voltage on the deflecting stages had to be large compared to the output of the low power oscillator, and it was desireable to have an undistorted sine wave signal across the R.F. plates, a resonant circuit was used. The capacitance across the R.F. plates was approximately 5 pfd. A coil consisting of twenty turns of copper wire on a half inch diameter form, was connected across the R.F. plates, and resonated at 15Mc. The balun, in this case, was terminated with a single turn of wire one inch in diameter, coaxial with the previous coil. A grid dip oscillator, loosely coupled to the input end of the cable system, was used to verify that the correct impedance matching had been achieved.

Reproduced with permission of the copyright owner. Further reproduction prohibited without permission.

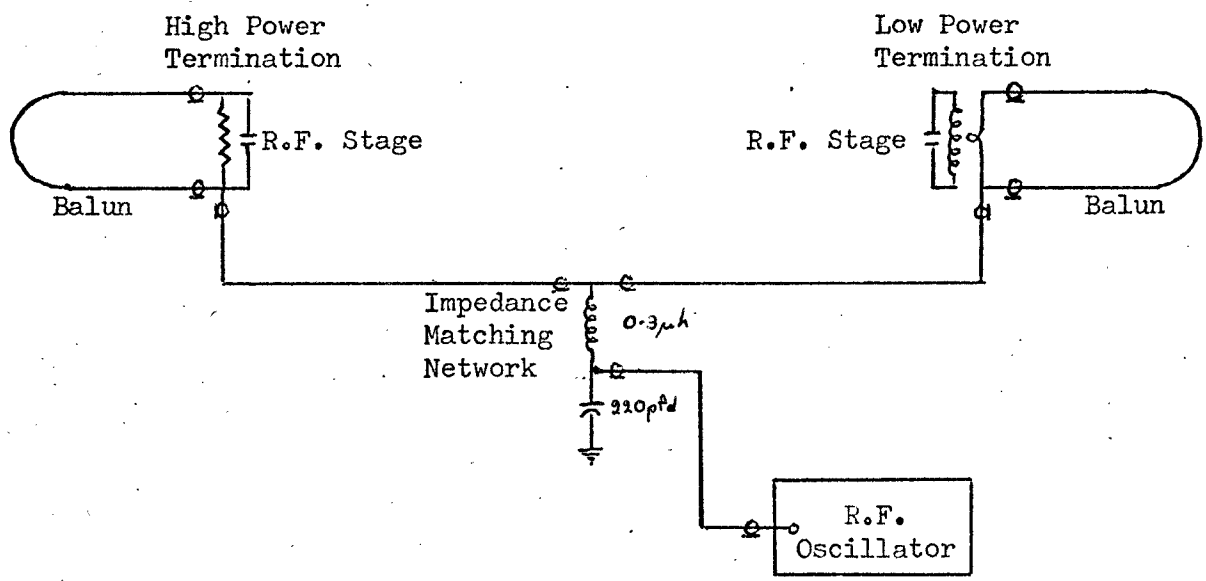

Figure VI. R.F. Distribution System

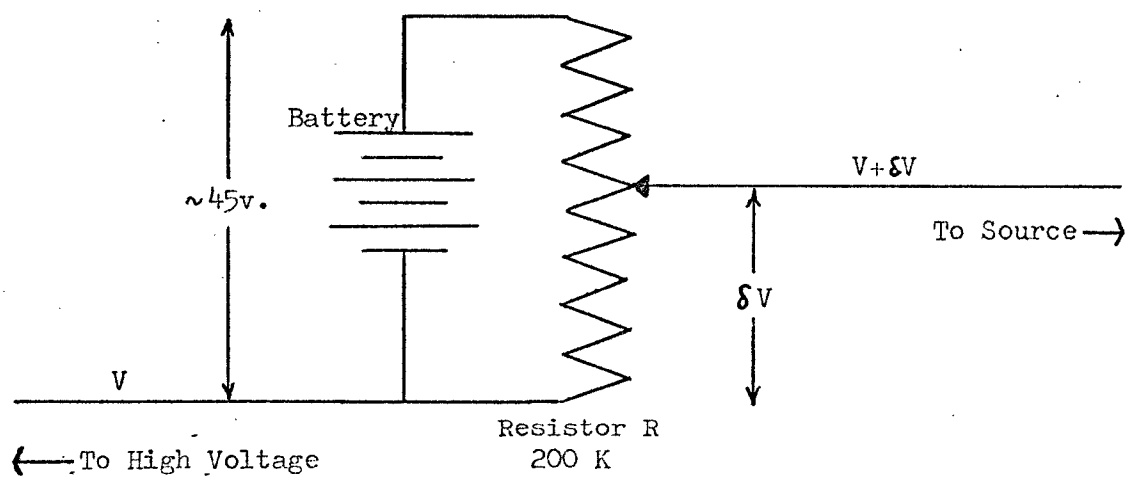

Figure VII. Slow Voltage Sweeping Circuit

Reproduced with permission of the copyright owner. Further reproduction prohibited without permission.

D. High Voltage Systems

The ion beams used in the instrument were produced in a surface ionization source. In such a source, a salt (in the present case $RbSO_4$) of the required ions is coated on a filament. Positive ions are emitted from the surface when the filament is heated to approximately 900°C. These ions are extracted from the source through a narrow slit and accelerated between the source slit and a ground slit by a Fluke 430A high voltage power supply. This supply has a stability of 0.005% per hour.

In order to obtain mass spectra with voltage sweeping, two techniques were employed. The simplest of these consisted of a slow voltage sweeping system in which the high voltage could be varied by about 0.5% in a period of half a minute. Figure VII is a schematic of the slow voltage sweeping circuit. The resistor R, a 200KΩ helipot driven by a 25 rpm. reversible motor, Borg 1003-4SY, is connected across a 45v. battery. The high voltage is connected to one side of the helipot and the ion source to the moveable contact. Thus the voltage appearing on the source is given by $V+\delta V$ where δV varies from zero to 45v. as the moveable contact is swept across the resistor.

As the voltage is swept in this system, particular masses will be detected when the source voltage satisfies Eq. I-2. The frequency applied to the R.F. stages is kept constant. The output of the detector is recorded on a strip chart, thus allowing the voltage separation of the mass peaks to be determined.

A fast voltage sweeping circuit was also tried, which permits the display of the mass peaks on an oscilloscope. Figure VIII is a block

Reproduced with permission of the copyright owner. Further reproduction prohibited without permission.

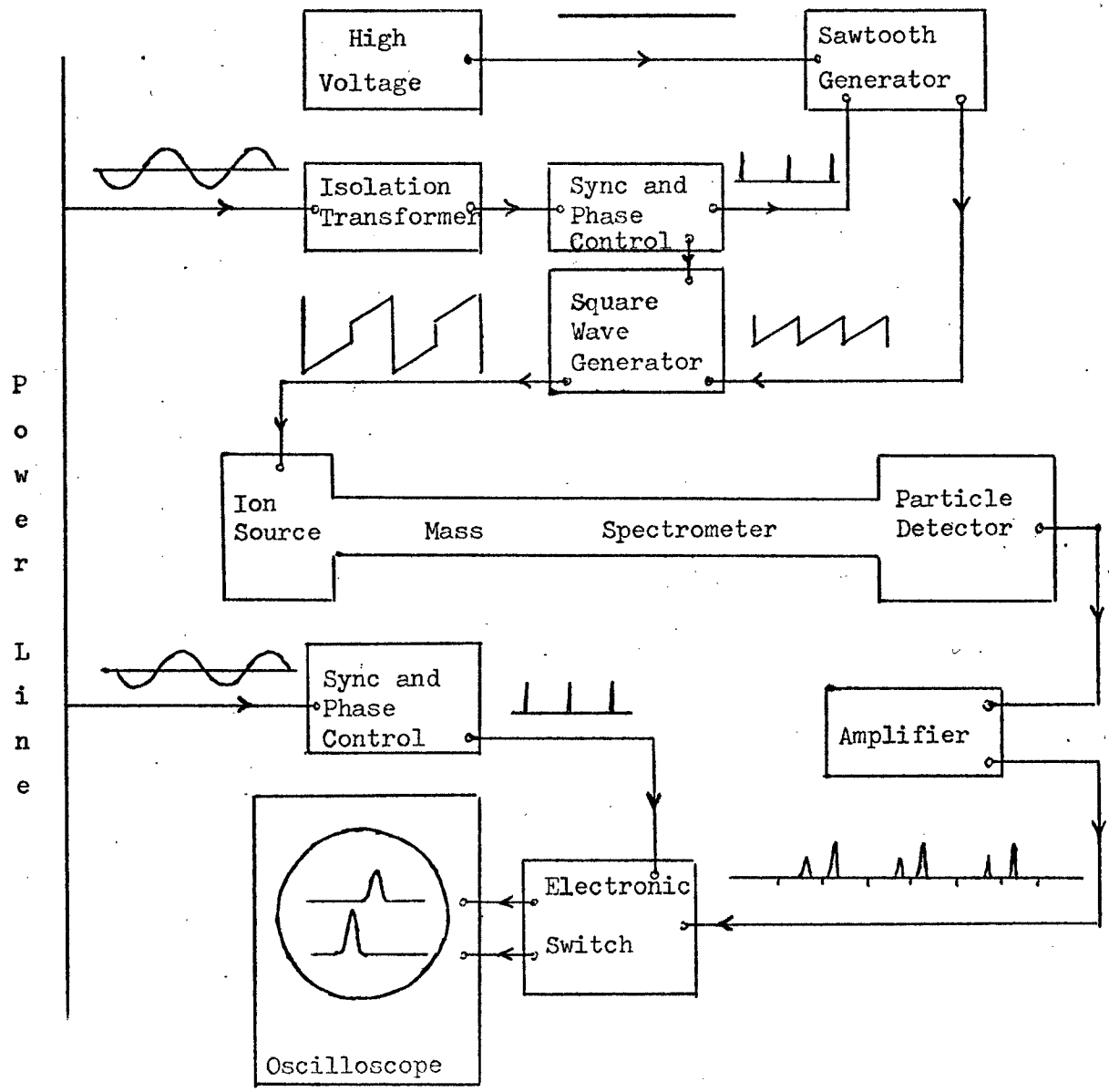

Figure VIII. A block diagram of the fast voltage sweeping circuits. The sawtooth generator superimposes a variable amplitude sawtooth onto the high voltage. This signal is fed into a variable amplitude square wave generator. The sawtooth is twice the freqency of the square wave, and the two are phase-locked to produce the composite signal indicated. This signal is used as the accelerating voltage for the ion source. The output of the detector is fed via an amplifier, into an electronic switch that is phase-locked to the transitions of the sawtooth. The two outputs of the switch are displayed on a dual beam oscilloscope which sweeps in phase with the electronic switch. The power line is used as the master timing control by providing synchronizing signals to the circuits.

Reproduced with permission of the copyright owner. Further reproduction prohibited without permission.

diagram of this system. If an ion is detected for a particular high voltage V_1, then the addition of a 120 cps. sawtooth signal from the sawtooth generator, will sweep the high voltage through this peak one hundred and twenty times a second. A second mass peak which is detected at V_2 may be treated in a similar manner. To make an accurate comparison of the two masses, a 60 cps. square wave of amplitude approximately equal to V_2-V_1 may be superimposed on the sawtooth voltage at V_1. Now the high voltage will alternately sweep through the two mass peaks. If the output of the detector is displayed on a dual beam oscilloscope in such a manner that each beam displays alternate 120th of a second periods, the display of each beam will correspond to one of the two mass peaks. The amplitude of the square wave can now be adjusted to bring the two peaks into vertical coincidence, at which time the amplitude of the square wave will be equal to the voltage separation of the two mass peaks.

E. Particle Detection

A low resolution, approximately one part in thirty, magnetic mass analyser was employed in such a manner that only the ions in a desired mass range could reach the detector. The magnetic field for the analyser is produced by a permanent magnet, and the magnetic field intensity varied by means of an adjustable shorting bar across the poles. Ions in the desired mass range are detected by a Bendix 306 Windowless Photon Detector. The output of this detector is measured by a Keithley 417 High Speed Pico-ammeter. In the case of fast voltage sweeping the output is fed into an amplifier and associated circuitry as shown in figure VIII. The output of the pico-ammeter is recorded on a Bausch and Lomb V.O.M.5 Strip Chart Recorder.

Reproduced with permission of the copyright owner. Further reproduction prohibited without permission.

CHAPTER IV

EXPERIMENTAL RESULTS

A. Slow Voltage Sweeping

The motor used to drive the helipot in the slow voltage sweeping circuit is self reversing, so that the high voltage is alternately increased and decreased by approximately 45v. causing the recording on the strip chart to repeat itself every minute or so. This provides a built in calibration for the recording since the voltage separation between every second peak of the same mass, providing that the mass peak appears only once in the interval δV, is equal to $2\delta V$. Then, because the voltage sweep is linear, a simple ratio of lengths can be used to determine the peak separations or widths. In figure IX the voltage, $2\delta V$, is 92v. since the actual δV provided by the sweeping circuit was 46v. The width of the of the peak indicated is, by calculation, 6.2v. This corresponds to a resolution of one part in three thousand. The theoretical resolution for this recording is one part in four thousand. The large peaks are due to Rb^{85} and the small ones to Rb^{87}.

B. Fast Voltage Sweeping

The circuit for fast voltage sweeping was built and tried on the mass spectrometer. However the technique was not employed extensively. There are two reasons for this. Firstly, the resolution of the instrument is not easily determined from the display on the oscilloscope since this requires a precise knowledge of the amplitude of the sawtooth in the high voltage circuit. This work is concerned with the preliminary operation

Reproduced with permission of the copyright owner. Further reproduction prohibited without permission.

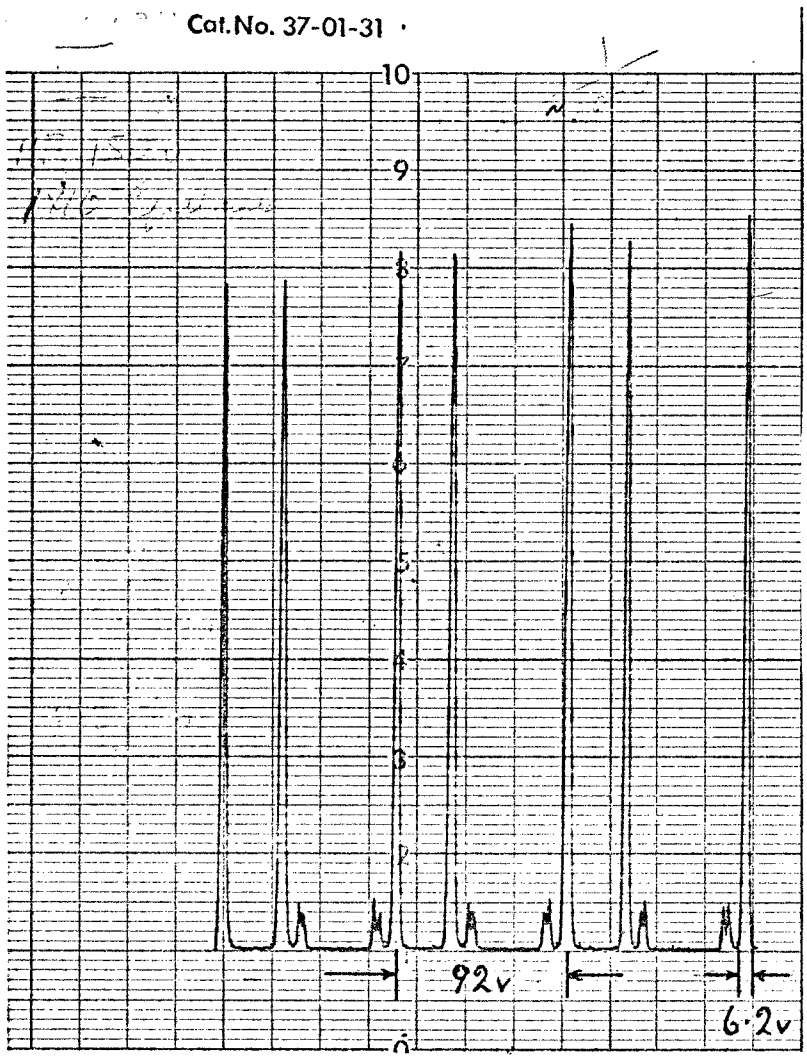

Figure IX. Recorder Trace for Slow Voltage Sweeping

177770

UNIVERSITY OF WINDSOR LIBRARY

Reproduced with permission of the copyright owner. Further reproduction prohibited without permission.

of the spectrometer, thus making an easy determination of the resolution almost a necessity. Secondly, it was found that the sawtooth generator and possibly the square wave generator were picking up some A.C. noise with the result that the peaks displayed on the oscilloscope were unsteady, jumping back and forth over a small range.

C. Frequency Sweeping, High Power Oscillator

The frequency sweeping with the high power oscillator proved to be the most convenient for the preliminary work because of its wide range. Figure X is a recording of a frequency sweep over a range greater than one megacycle centred at 15Mc. Although the resolution is not too high in this particular recording, it does show a good stability and the wide range over which the cable system can be used. It should be mentioned that the high power oscillator was also used during the slow voltage sweep for the results shown in figure IX.

The particular recording in figure X shows how the mass peaks for different masses overlap at high n numbers. The small peak has a lower repetition frequency than the large one, thus the small peak appears to emerge from under the large one on the left hand side, move between two large peaks, and then go back under a large peak from the right hand side, as the frequency increases.

D. Frequency Sweeping, Low Power Oscillator

The low power oscillator using the resonant circuit to drive the R.F. plates, had, in contrast to the high power oscillator, a working frequency range of only approximately 100Kc. However in this range the mass peaks are quite good showing a resolution of one part in six thousand.

Reproduced with permission of the copyright owner. Further reproduction prohibited without permission.

Reproduced with permission of the copyright owner. Further reproduction prohibited without permission.

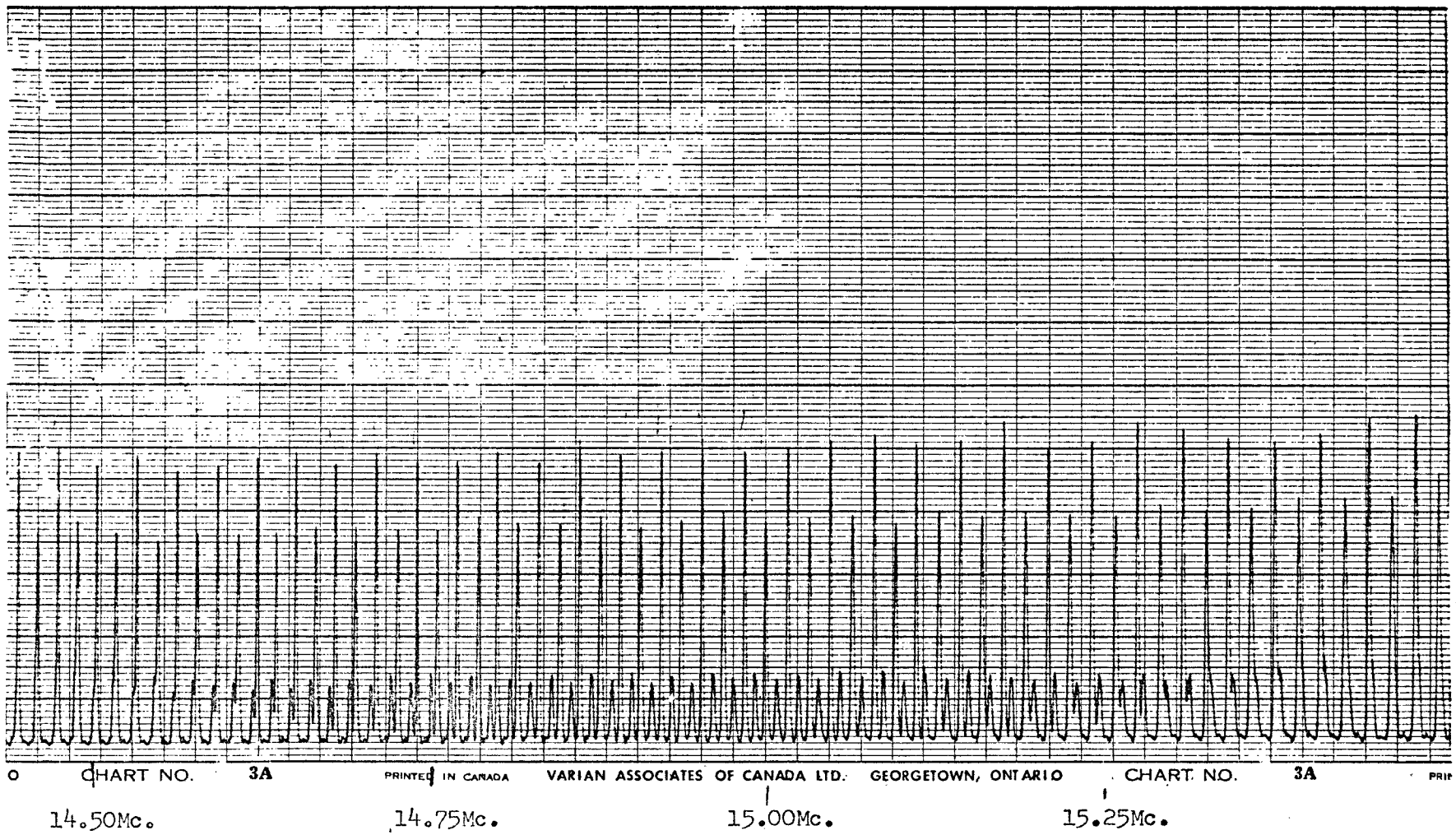

Figure X. Recorder Trace for Frequency Sweeping with the High Power Oscillator

Reproduced with permission of the copyright owner. Further reproduction prohibited without permission.

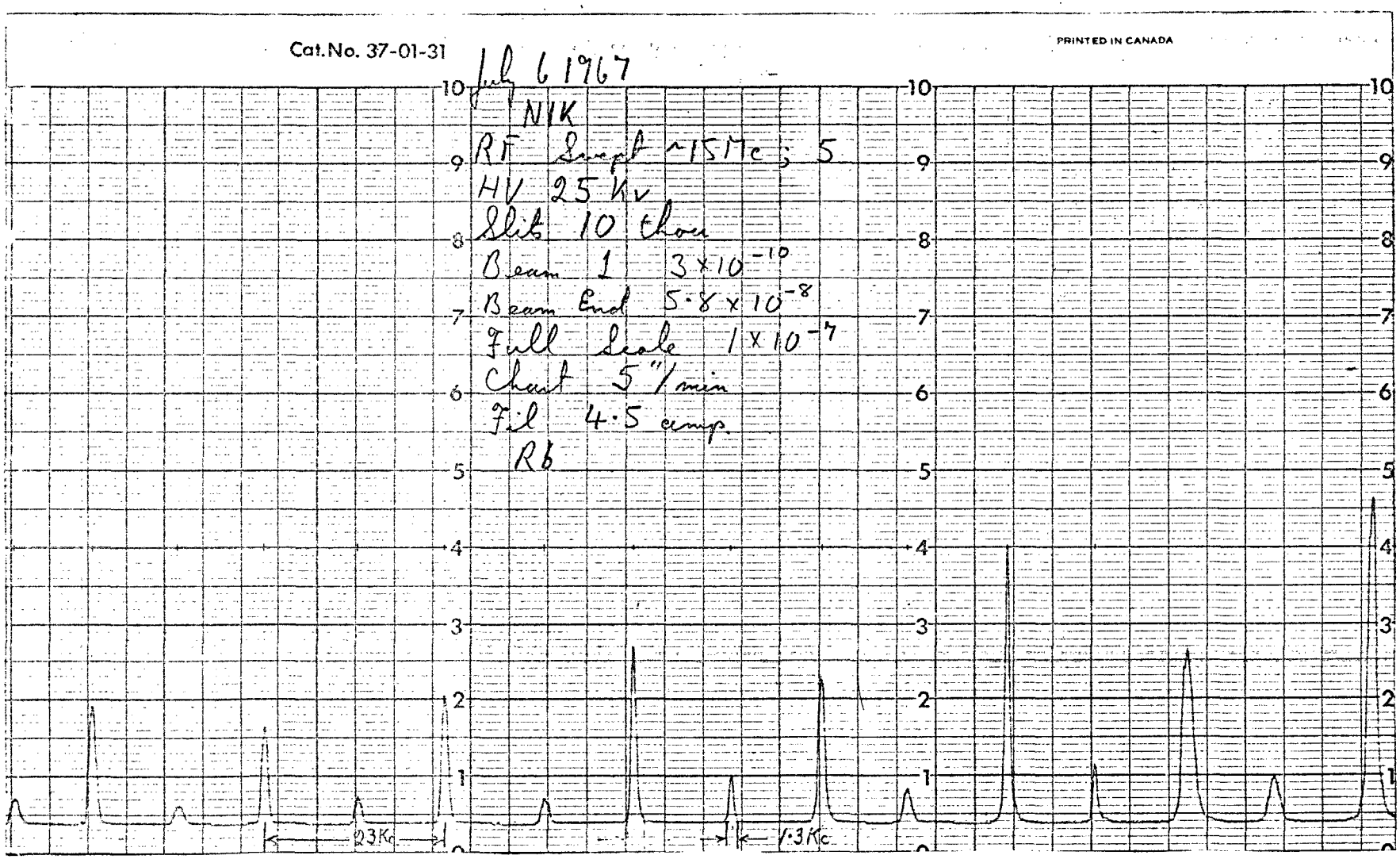

Figure XI. Recorder Trace for Frequency Sweeping with the Low Power Oscillator

Figure XI is a recorder tracing of a frequency sweep using the low power oscillator in which the peaks to the left are occuring at resonance and the ones to the right are off resonance. It is impossible to measure the voltage on the R.F. plates when the resonant circuit is employed since this would disturb the resonance. The amplitude of the R.F. voltage is estimated to lie in the range 50 to 100v.

If the R.F. voltage is increased, the peaks start to broaden and split as can be seen in figure XII. This recorder tracing was taken at the same time as that in figure XI, the only difference between the two being an increase in the R.F. voltage for figure XII. These effects were also observed when the high power oscillator was employed if the R.F. voltage was increased much beyond 50v. In figure XII the odd peaks for both of the masses, Rb^{85} and Rb^{87} , have split and the even peaks for both of the masses are broadened.

E. General Results

It was mentioned in Chapter I that a low resolution magnetic mass analyser was used so that only a small mass range could reach the detector. Figure XIII is a recorder trace of the output of the mass spectrometer without the magnetic mass analyser, but with the particle detector mounted directly behind slit S_6. Since there several mass peaks present, it is difficult to make any accurate measruements of the resolution or the peak separations.

The experimental verification of the different mass resolution for even and odd peaks can be seen in figure XIV. Both of the rubidium mass

UNIVERSITY OF WINDSOR LIBRARY

Reproduced with permission of the copyright owner. Further reproduction prohibited without permission.

Figure XII. Recorder Trace of Frequency Sweeping for the Low Power Oscillator showing Peak Splitting

Reproduced with permission of the copyright owner. Further reproduction prohibited without permission.

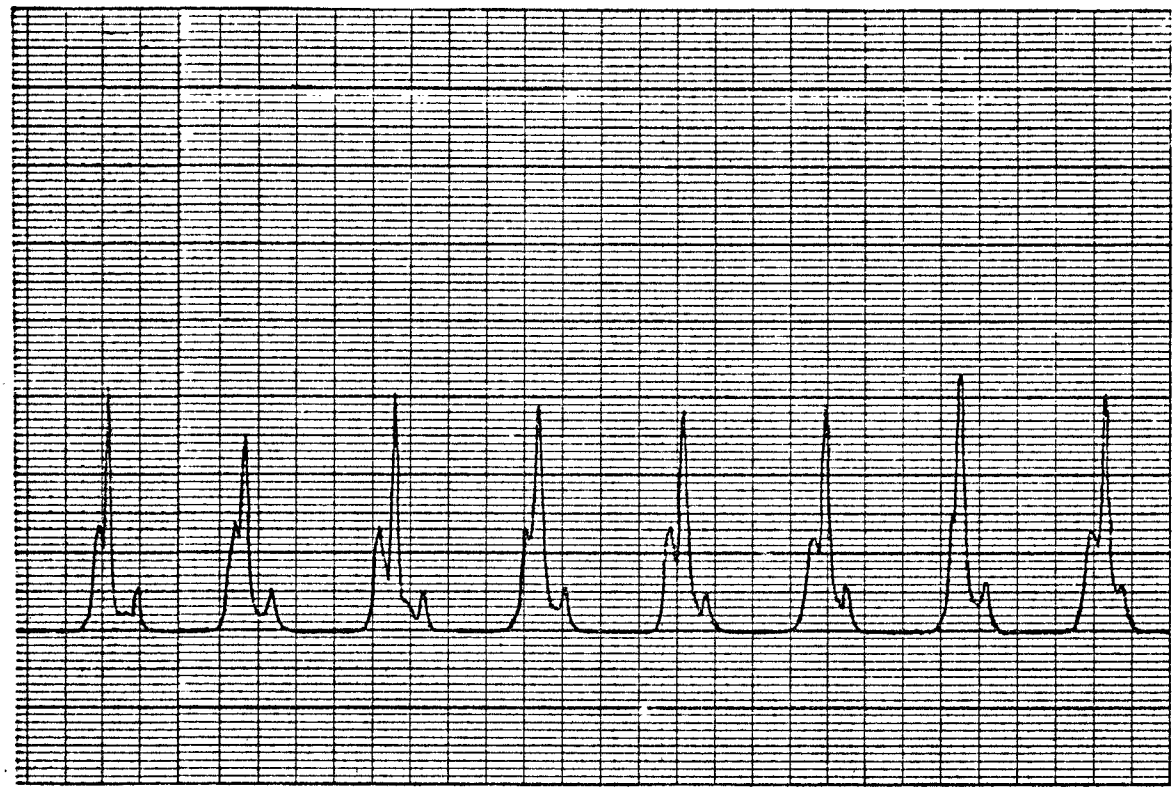

Figure XIII. Recorder Trace of Mass Peak Overlapping

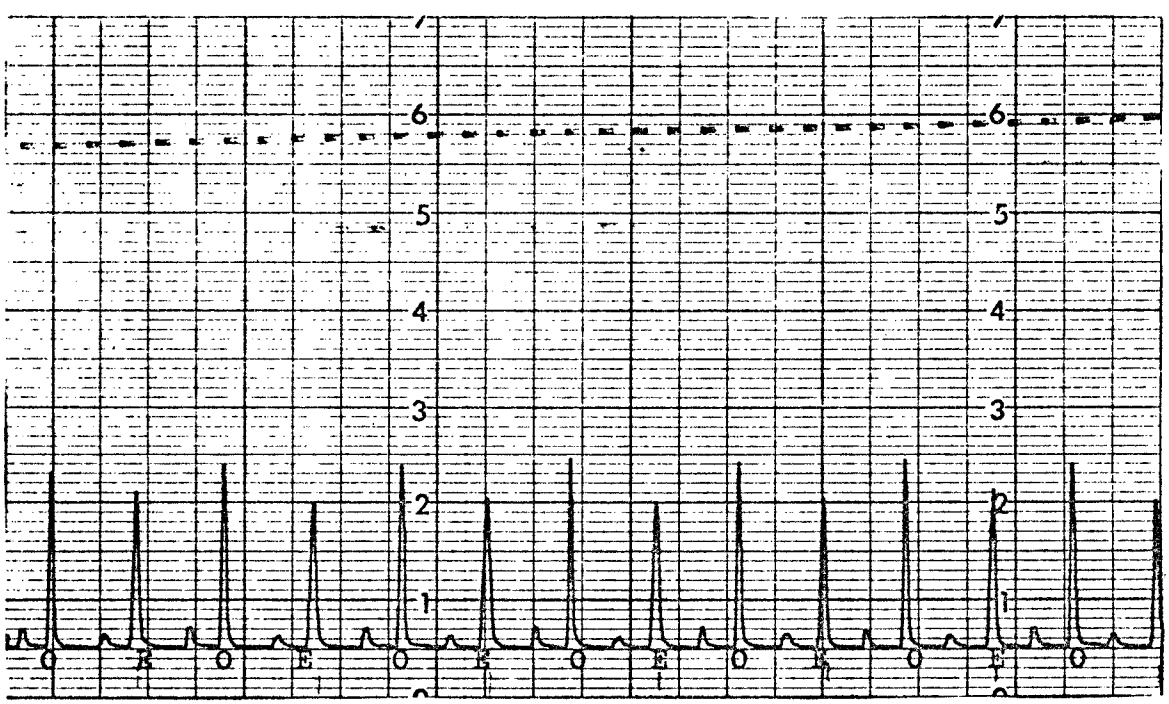

Figure XIV. Recorder Trace Showing the Different Mass Resolution for Even and Odd n Numbers

Reproduced with permission of the copyright owner. Further reproduction prohibited without permission.

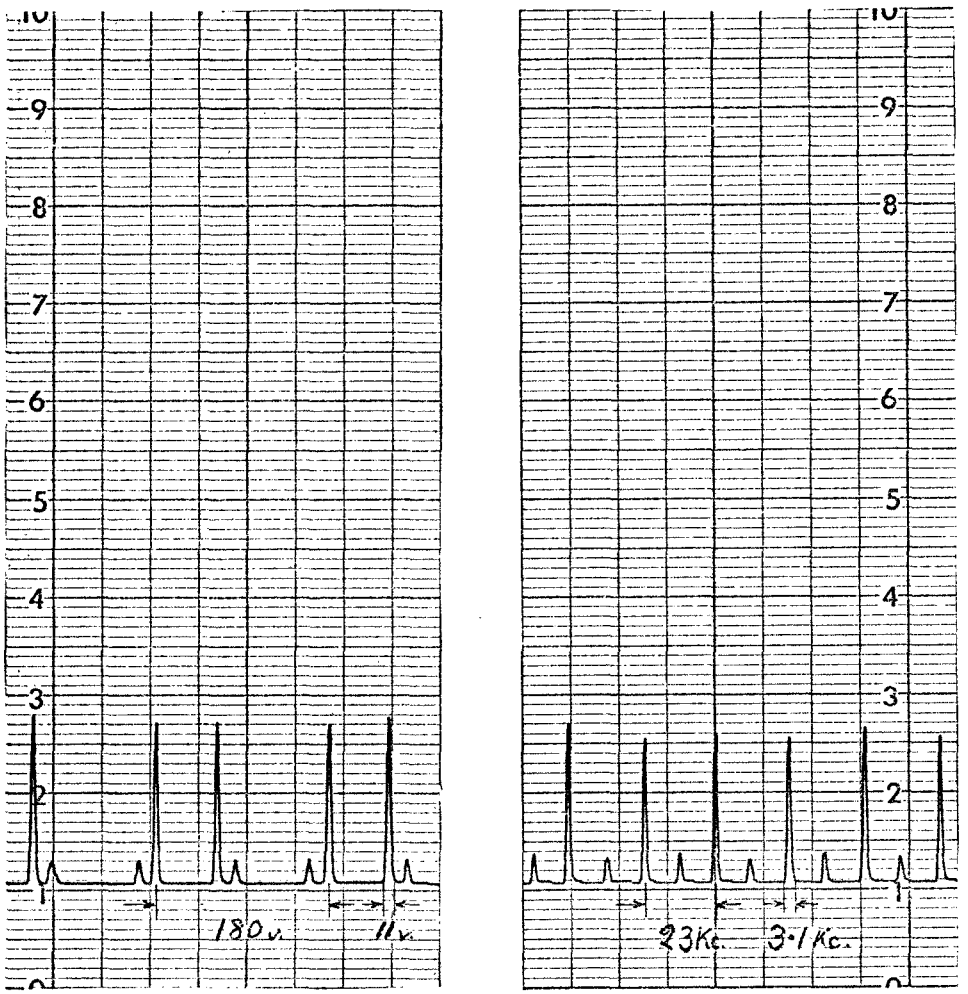

Voltage Sweep

Frequency Sweep

Figure XV. Recorder Traces for a Voltage and a Frequency Sweep Showing Comparable Resolutions under the same Conditions

Reproduced with permission of the copyright owner. Further reproduction prohibited without permission.

peaks are present, but due to its greater intensity, the Rb^{85} peak shows the effect better. The even n number peaks have been marked with an E and the odd peaks with an O. The widths of the even and odd peaks are in the ratio of approximately three to two. This is in agreement with the theory developed to explain this effect.

Figure XV shows a slow voltage sweep and a frequency sweep using the high power oscillator. These two sweeps were taken one after the other so that the conditions are the same for both sweeps. The voltage sweep gives a resolution of one part in twenty two hundred, while the frequency sweep gives a resolution of one part in twenty four hundred. Since the resolutions are approximately the same, it indicates that the frequency, in the voltage sweep, is as stable as the voltage, in the frequency sweep.

Reproduced with permission of the copyright owner. Further reproduction prohibited without permission.

CHAPTER V

DISCUSSION AND CONCLUSION

The new Time of Flight Mass Spectrometer shows significant improvement over the one used by Lum, in stability, reliability, and ease of operation. However, with the present instrument a resolution of at least one part in twenty thousand should be possible, since the voltages that have been applied to the deflecting plates are only a small fraction of those that can be supplied by the oscilators. As was seen in IV,E if an R.F. voltage greater than about 50v. was applied to the deflecting plates, the odd mass peaks started to split while the even mass peaks broadened. These effects are not fully understood at present and only possible causes for them will be advanced in this discussion.

It is thought that the broadening of the even mass peaks may be due to a component of the R.F. electric field in the direction of the ion beam. If this is the case, then as the ion beam passes through an R.F. stage part of it will receive an acceleration in the direction of the beam while the other part will receive a deceleration. The net effect will be cumulative for the even mass peaks and cancel for the odd mass peaks. Thus the even mass peaks will tend to become broader than is predicted by theory while the odd mass peaks will continue to increase in resolution as the R.F. voltage is increased.

If there is a harmonic distortion of the R.F. signal, then instead of having half periods that are all equal to each other, it is possible to have two different half periods in each cycle. This distortion will

Reproduced with permission of the copyright owner. Further reproduction prohibited without permission.

not affect the even mass peaks, since an even number of consecutive half periods will always yield the same timing interval no matter where they are taken. However, an odd number of half periods can yield two different timing intervals depending on where the initial half period is taken. Thus, this type of distortion will cause the odd mass peaks to split if the difference between the two timing intervals is sufficiently large, while the even mass peaks will not be affected.

Although a high resolution has not been achieved in the preliminary work due to the peak splitting and broadening, it is felt that the instrument is capable of a much higher resolution once the exact cause of these effects has been found and corrected.

Reproduced with permission of the copyright owner. Further reproduction prohibited without permission.

BIBLIOGRAPHY

Duckworth, H.E. (1958). Mass Spectroscopy, Cambridge University Press.

Lum, R.M. (1964). A New Time of Flight Mass Spectrometer, Master of Science Thesis, University of Windsor.

Inghram, M.G. and Hayden, R.J. (1954). Mass Spectroscopy, National Research Council.

Reproduced with permission of the copyright owner. Further reproduction prohibited without permission.

VITA AUCTORIS

1943 - Born April 10, Birmingham, England

1954 - Took up residence in Windsor, Ontario

1957 - Graduated from Prince of Wales Public School

1962 - Graduated from Patterson Collegiate Institute

1966 - Graduated from University of Windsor with B.Sc. (Hon.) in Physics

Reproduced with permission of the copyright owner. Further reproduction prohibited without permission.